

601120

2 of 3

WAL TR III.2/20-6

37-P \$1.00

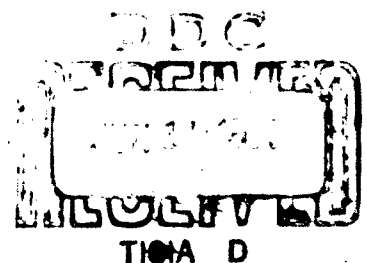
BASIC PARAMETERS
OF METAL BEHAVIOR
UNDER HIGH RATE FORMING

final report to

U. S. ARMY MATERIALS
RESEARCH AGENCY

20050513057

Best Available Copy



Filing Subjects:

1. Explosive forming
2. Dynamic behavior of metals
3. High rate deformation
4. Strain rate effects

BASIC PARAMETERS
OF
METAL BEHAVIOR UNDER HIGH RATE FORMING

by

P. C. Johnson
B. A. Stein
R. S. Davis

FINAL REPORT

to

U. S. ARMY MATERIALS RESEARCH AGENCY
WATERTOWN, MASSACHUSETTS

October 1962 - December 1962

Technical Report No. WAL TR 111.2/20-6

Report No. WAL TR 111.2/20-6
OMS Code 5010.11.8430051
D/A Project 5B93-32-004
Contract No. DA-19-020-ORD-5239
Boston Procurement District, U. S. Army

C-63080

The findings in this report are not to be construed
as an official Department of the Army position

DISPOSITION INSTRUCTIONS

Destroy; do not return

DDC AVAILABILITY NOTICE

Qualified requesters may obtain copies
of this report from DDC

ABSTRACT

This report summarizes the results of the investigations made in this program. These include measurement of high strain rate plastic flow properties and ductility in a uniaxial, homogeneous stress system and a study of deformation mechanics in high energy rate forming operations.

Presented here for the first time are the results of a study made on the energy transfer process at a liquid-metal interface. It was found that separation of the liquid and the metal occurs only after a number of wave reflections have taken place. Finally, the report concludes with a discussion of some of the major problems associated with high energy forming processes which remain to be investigated before these processes can be adequately understood.

TABLE OF CONTENTS

	<u>Page</u>
List of Figures and Tables	vii
I. INTRODUCTION	1
II. PLASTIC FLOW BEHAVIOR AT HIGH STRAIN RATES	2
III. DUCTILITY AT HIGH STRAIN RATES	15
IV. THE HIGH ENERGY RATE FORMING PROCESS	19
V. FUTURE EFFORTS	30

LIST OF FIGURES AND TABLES

<u>Figure No.</u>		<u>Page</u>
1	The Expanding Ring and Its Stress System	5
2	Ring and Core Assembly	7
3	Stress-Strain Results-99.99% Aluminum	10
4	Stress-Strain Results-7075-T6-Aluminum	11
5	Stress-Strain Results-304 Stainless Steel	12
6	Stress-Strain Results-Armco Iron	13
7	Stress-Strain Results-Titanium-6 Aluminum-4 Vanadium	14
8	Experimental Apparatus Interface Energy Transfer	21
9	Experimental Cell	23
10	Schematic of Velocity Pickup	25
11	Velocity Pickup Apparatus	26
12	Water-Aluminum Transfer	29
13	Aluminum-Aluminum Transfer	29
14	Wave Reflection Trace	29
<u>Table No.</u>		
I	Uniform Elongation to Failure	16
II	Hardness of 304 and 4340 Steels - V. P. N.	17

I. INTRODUCTION

The application of high strain rate techniques to the forming of metal parts has received considerable attention in recent years. These techniques are currently in limited use for the production of parts, primarily in the aerospace industry. High energy rate forming has shown itself particularly advantageous for certain complex shapes and relatively short runs. The art of forming at high rates has developed largely as a result of trial and error approaches to the problem. It is not yet possible to design the forming operation from first principles because of a lack of understanding of the behavior of materials at high rates of strain.

The process by which parts are formed at high rates of strain is an exceedingly complex one because of the multiplicity of the factors which are involved. These factors can be broken down into two areas which are amenable to independent investigation. The first of these is concerned with the effects of strain rate on the plastic flow behavior of materials in the microscopic sense. That is, it is concerned with the effect of strain rate on the mechanisms of dislocation generation and motion and the effect that changes in these mechanisms have on the plastic flow curve and final properties of the deformed material. The second general area of interest is that of the deformation mechanisms involved in the process in a more macroscopic sense. Of primary importance in this area are the generation, propagation, and interaction of the plastic waves which accomplish the deformation in an actual forming operation. The deformation mechanisms are closely related to the process design variables such as the energy source and configuration, transfer medium, energy transfer to the blank, and die design.

This program has consisted of the investigation of some of the above parameters using both experimental and theoretical approaches. Our investigations have been concentrated in the following areas:

1. Measurement of plastic-flow curves at high strain rates.
2. Measurement of ductility at high strain rates.
3. Investigation of the energy transfer process at a fluid-metal interface.
4. Development of an understanding of high energy rate forming processes on the basis of information produced by our investigations and the investigations and experiences of others in this field.

II. PLASTIC FLOW BEHAVIOR AT HIGH STRAIN RATES

A. BACKGROUND

The first step in the development of a basic understanding of high energy rate forming processes must be a knowledge of the plastic flow behavior of materials at high strain rates. Our current understanding of the mechanical properties of materials is largely dependent on observations of their deformation at very low rates of strain. The standard tensile test has provided the bulk of the data on which this understanding is based. This technique is useful at low rates of strain because it can be designed to provide a section of material which is large enough for convenient measurement and over which the stress system is simple and uniform.

The standard tensile test loses a great deal of its simplicity and usefulness at higher rates of strain. Above a certain strain rate the stress system loses its homogeneity because the time required for the stress to propagate, as waves, from the point of application of the load to the other portions of the specimen, becomes comparable to the rate at which the stress is changing. Therefore, studies of high rate deformation under these conditions must necessarily include the determination of the propagation characteristics of stress waves under the conditions of the test.

The propagation characteristics of elastic stress waves in the rod-like specimens which are generally used for tensile testing can be adequately and accurately described in terms of the elastic constants for the material. A brief description of elastic wave propagation was included in the First Yearly Report on this program (WAL TR 11.2/20). By contrast, no accepted theory for plastic wave propagation exists for this kind of system.

There are two general theories which have been developed to describe the propagation of plastic waves down impacted bar specimens. The first of these, the strain rate independent theory, was developed separately by T. von Karman,¹ G. I. Taylor,² and K. A. Rakhmatulin.³ This theory assumes that the material behavior is strain rate independent, and describes the wave parameters in terms of the quasi-static plastic flow parameters of the material. The second of these theories is the strain rate dependent approach of L. E. Malvern.⁴ The material is treated as a visco-elastic medium which deforms according to a plastic flow law involving stress, strain, and strain rate of the form

$$E \dot{\epsilon} = \dot{\sigma} + g(\sigma, \epsilon)$$

Malvern used a linear form of the strain rate function $g(\sigma, \epsilon)$. That is, he assumed that the strain rate is proportional to the excess of stress over the stress at the same strain in a quasi-static test. One of the advantages of the visco-elastic treatment is that the function $g(\sigma, \epsilon)$ can be given whatever form is necessary to conform to experimental observations.

Unfortunately, neither theory has proved capable of explaining all the experimental observations on the propagation of plastic waves down impacted rods. A great deal of experimentation has been carried out on the bar, notably by J. F. Bell⁵ and by E. A. Ripperger and C. H. Karnes.⁶ Despite very sophisticated measuring techniques, deviations from the strain rate independent theory have not been adequately explained in terms of a quantitative strain rate effect.

For the strain rate regime in which wave propagation effects become important, a great deal of work has been done in systems where the wave problem is neglected and results are presented as average values. This approach has been responsible for a large part of the existing data on the effect of strain rate on the mechanical behavior of materials.

Most of this kind of experimentation has involved measurement of the energy absorbed by specimens impacted in compression. The mean strain is measured on the specimen after impact, and the mean stress and mean strain rate are calculated from energy change measurements on the impactor. Although this kind of experiment does not require consideration of wave propagation, stress waves are present, and the experiment simply measures the average effect of these waves. A detailed survey of the work which has been carried out using these techniques is included in the First Yearly Report (WAL TR 11.2/20). In general, this "averaging" work has shown moderate increases in the yield and the work-hardening rate with increased strain rate. There are, however, considerable variations reported which fall within this general trend.

An interesting combination of averaging wave techniques is currently being used by Hauser, Simmons, and Dorn⁷ for high strain rate behavior studies. It is a modified version of the "thin wafer" technique suggested by Kolsky⁸ for the indirect measurement of stress and strain during the plastic deformation of a dynamically loaded specimen. A short tubular section of a relatively soft material is sandwiched between two long, relatively hard metal tubes. A compressor stress wave, whose intensity is below the yield strength of the hard bars and above the yield strength of the soft specimen, is induced in one end of the assembly by impact with a high-speed ram. Strain-time measurements in the elastic bars on both sides of the soft specimen provide indirect data on the average stress and average strain in the specimen. By varying the intensity of the impact and the specimen thickness, they are able to vary the average strain rate over a range of 50 to 12,000 per second. On high purity aluminum they observe an increase in

flow stress with increasing strain rate. The amount of the increase in stress is greater the greater the strain level. At strain rates near 10^4 per second, their results indicate that the strain rate versus stress curve is approaching an asymptote. That is, the stress required to reach a given level of strain at these strain rates is approaching infinity. This latter result, however, is probably caused by the lateral constraints imposed on the specimen by the elastic bars for the thin specimens and short times involved at these highest strain rates.

B. EXPERIMENTAL APPROACH

The only ideal solution to the problem of measuring high rate deformation is a test in which there is no wave propagation and the stress system is therefore uniform. Only in the absence of waves can a test be made which can be compared directly with the standard tensile test used at lower strain rates. We have devised and used a system which provides dynamic stress-strain data on a specimen which is deformed by an essentially uniaxial, homogeneous stress system.

The technique involves the observation of a freely expanding ring of the material being tested. A ring of small cross section is pressed onto a cylindrical core which has high explosive packed into a hole along its axis. After detonation, the ring acquires an initial radial velocity by trapping a portion of the compression shock wave emanating from the center of the core. Contact between the ring and core is broken when the tensile wave reflected from the outside surface of the ring arrives at the ring-core interface. At this instant, the ring has acquired its total energy; no subsequent radial forces act on the ring. There are, of course, radial velocity gradients as long as radial waves exist in the ring. However, their velocity is much higher than that of the ring, and the radial velocity becomes uniform before any appreciable ring motion takes place. Thus, for a symmetrical system, all sections of the ring have a uniform velocity at any instant of time during the deformation.

Since the cross-section of the ring is small relative to the diameter, release waves propagating inward from the surfaces of the ring travel only short distances. There are, therefore, no stresses in the plane of the cross-section; the only stresses are normal to this plane, i. e., hoop stresses. Since the velocity of the ring is uniform around its circumference, the hoop stresses are uniform, and no waves are initiated or propagated in the circumferential direction. The ring thus represents a freely expanding specimen being decelerated only by a uniaxial stress which is everywhere homogeneous in the direction of major strain. The ring is thus a very close analogue of the standard tensile test.

The kinetic behavior of the expanding ring can be related to the circumferential stress in the ring by conservation of energy requirements. Conservation of mass implies that the density, ρ , is constant. This is not strictly true

in the elastic region, but the deviation can be taken into account by use of the dynamic Young's modulus in this region.

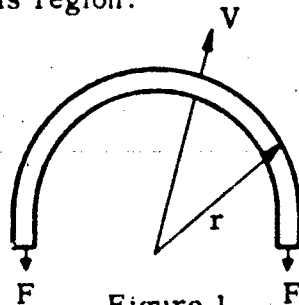


Figure 1

Conservation of energy requires that the kinetic energy lost by the ring go into strain energy

$$\Delta \left(\frac{1}{2} m v^2 \right) = F (\pi \Delta r)$$

for the half-ring

$$\frac{1}{2} m \left(v_0^2 - v^2 \right) = F \pi (r - r_0)$$

Differentiating with respect to time, where $\dot{r} = \frac{dr}{dt}$ and $\ddot{r} = \frac{d^2r}{dt^2}$

$$\frac{1}{2} m 2 v \dot{v} = -F \pi \dot{r}$$

Since $v = \dot{r}$, $\dot{v} = \ddot{r}$, then $\frac{1}{2} m 2 \ddot{r} = -\pi F$

$m = \pi r A \rho$ for the half-ring, where A is the ring cross section and ρ is the density

$$F = \sigma A$$

$$\therefore \sigma = -\rho r \ddot{r}$$

or

$$\sigma = -\rho r r_0 \ddot{\epsilon} \quad (1)$$

Equation 1 gives the hoop stress as a function of the ring deceleration. The dynamic stress-strain relationship follows directly from the second differential of the strain-time relationship. This equation is an exact equation, provided the physical description of the expansion process is accurate.

It is possible to predict the strain-time behavior of a ring by solving Equation 1 above on the basis of an assumed stress-strain curve. The equation is more useful for this purpose in the form

$$E \epsilon + r_0^2 (\epsilon + 1) \rho \ddot{\epsilon} = 0 \quad (2)$$

where E is Young's modulus. The equation is difficult to solve for complex stress-strain relations. It has been solved, with examples, in the First Yearly Report (WAL TR 11.2/20) for three cases:

1. The case in which the initial ring velocity is not sufficient to exceed the elastic limit.
2. Plastic flow at a constant stress level, the yield stress (no work-hardening).
3. Plastic flow defined by a linear flow curve (constant work-hardening rate).

C. EXPERIMENTAL TECHNIQUE

The specimen assembly is shown in Figure 2. An explosive is packed into a blind hole whose diameter is varied to provide a range of initial velocities. The explosive is detonated at the open end of the hole by an electrical blasting cap, producing a shock wave which radiates out from the axis. The wave also has an axial component of motion toward the blind end of the hole; the magnitude of this component depends on the relative velocities of shock-wave propagation in the core and detonation in the explosive. The test ring is fitted tightly to the core against a shoulder. The standard ring size which has been used in this work is 2 inches in diameter with a 0.1 x 0.1 inch cross-section.

In general, the ring separates from the core because it traps the higher pressure portions of the shock wave. However, if a soft core material is used, the core may catch up to the ring as the ring decelerates. If this happens, the strain-time plot of the ring shows a second acceleration when the core hits it. Data obtained beyond this point are useless because additional energy is being supplied to the ring. The problem can be avoided altogether by choosing a core material having significantly higher yield and work-hardening values than the ring.

High speed photography has proved to be the best method for measuring the strain-time relationship of the expanding ring. The event takes place in 25 to 100 microseconds, depending on the material and initial velocity. Because

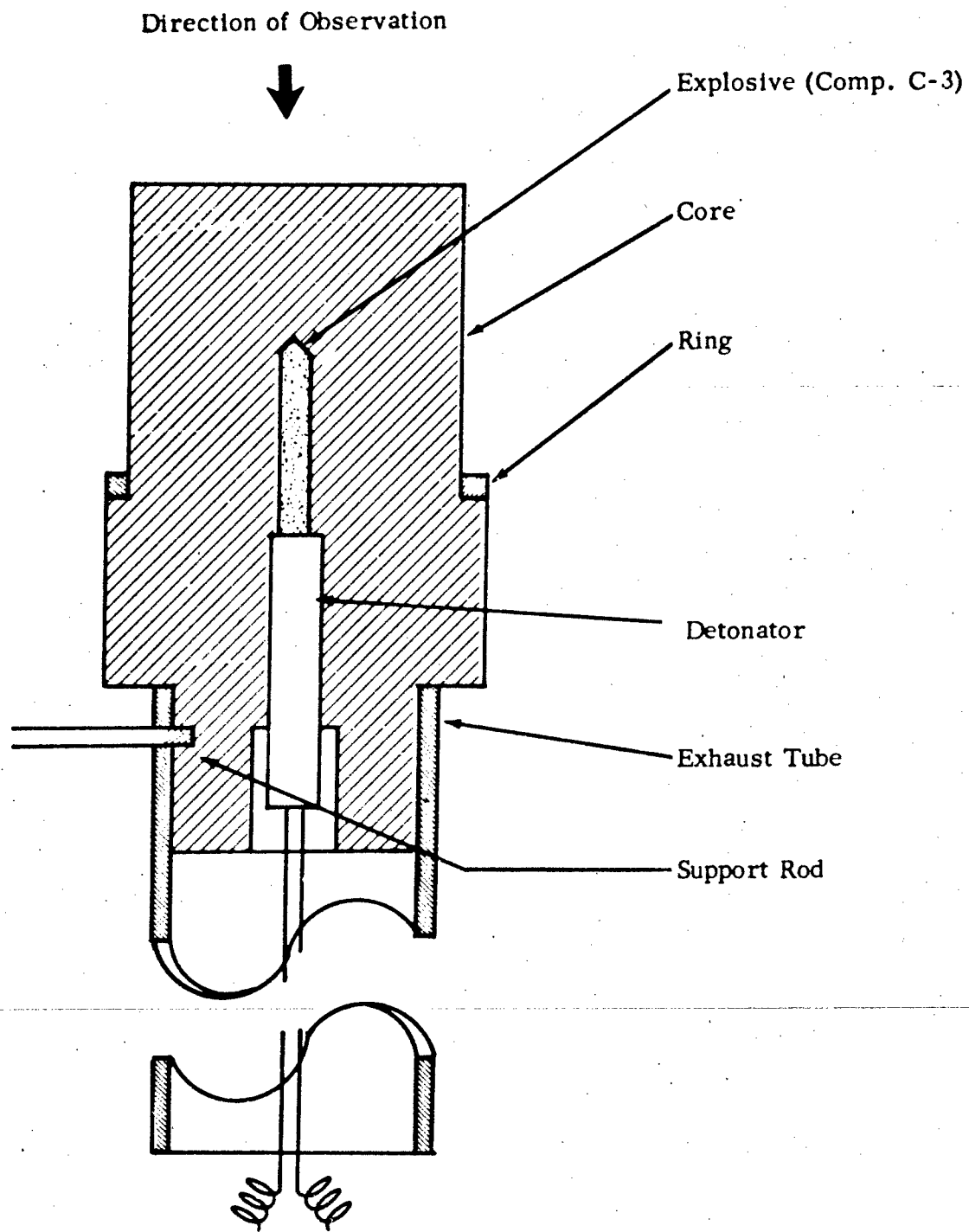


FIGURE 2 RING AND CORE ASSEMBLY

a second differential must be calculated from the data, it is necessary, in the interest of maximizing the accuracy, to record a reasonably large number of strain-time points as the ring expands.

The event is viewed along the axis of the core from the closed end. The blind hole and the exhaust tube prevent the detonation products from obscuring the image of the ring as it expands. The event is back lighted by an exploding tungsten wire and an appropriate optical system.

Two series of tests were carried out using the ring experiment, with slight differences in technique. The first series, on 99.99% aluminum, is treated in detail in the First Yearly Report (WAL TR 11.2/20), while the second series, on five metals, can be found in greater detail in the Fifth Interim Report (WAL TR 11.2/20-4). The first series was carried out using the facilities of the Ballistic Research Laboratory of the Aberdeen Proving Ground, while in the second series we made use of the personnel and facilities of Beckman & Whitley, Inc., of San Carlos, California.

D. DATA REDUCTION

The strain-time data for each test were obtained by measurement of the diameter of magnified image of the ring in an optical comparator. We used two methods to obtain strain rate and stress calculations from this data. In the first series, regression analysis was used to fit a curve of the form

$$\epsilon = a_0 + a_1 t + a_2 t^2 + a_3 t^3 + a_4 t^4$$

to the strain-time data. Subsequent computations of the first and second derivatives, the strain rate, and the stress, all as a function of strain, were carried out by the computer. The accuracy of our strain-time data in this first series was such that a polynomial strain-time relation such as that given above gave adequate fit to the data.

Our strain-time data were much more accurate in the second series due to refinement of the technique. As a result, we discovered that the dynamic behavior of the rings was too complex to be described by a simple polynomial expression. Instead of using analytical data reduction methods for this series, we calculated the strain rate and stress values from first and second derivatives obtained by graphical methods. Although this introduced the element of human judgment into the data reduction, a second independent treatment of the same data yielded strain rate and stress values within 10 percent of the first values. This is a reasonable accuracy in light of the changes in flow stress level as a result of the high strain rates which we measured in these tests.

The data reduction techniques are described in greater detail in the First and Fifth reports on this contract. These reports also contain error analyses for the two series of tests.

E. RESULTS

The results of our high strain rate plastic flow measurements are summarized in Figures 3 through 7. The dynamic stress-strain tests gave either a constant work-hardening slope or, at worst, an average flow stress (no work-hardening) within the accuracy of the technique. The high strain rate results are the average of a varying number of tests for each material. The tests on Armco iron gave results which fell into two distinct groups, depending on the initial strain rate. Both have been shown in Figure 6. The high strain rate curves are valid only above about 1 percent strain. The mean initial strain rates for each material are indicated in the figures. The strain rate, of course, decreases with increasing strain. The strain rate at the highest strain shown for each material is still 10^3 per second or higher.

The low strain rate flow curves are shown somewhat schematically as straight lines connecting the measured yield strength and the flow stress at the highest level of strain included on the figures. The departure from linearity on the actual curves is not great in the ranges of strain which are included. The low strain rate flow curve for titanium-6 aluminum-4 vanadium is given only up to the strain at its ultimate tensile strength.

The results of the initial series of tests on 99.99% aluminum are not included here. These can be found in detail in the First Yearly Report (WAL TR 11.2/20). The materials and their treatment are described in detail in the Fourth Interim Report (WAL TR 11.2/20-3). Included in this latter report also are the low strain rate properties of these materials, the raw strain-time data for each high rate test, and the equations of the high strain rate flow curves for each test. The second series of tests and the results are discussed in detail in the Fifth Interim Report (WAL TR 11.2/20-4).

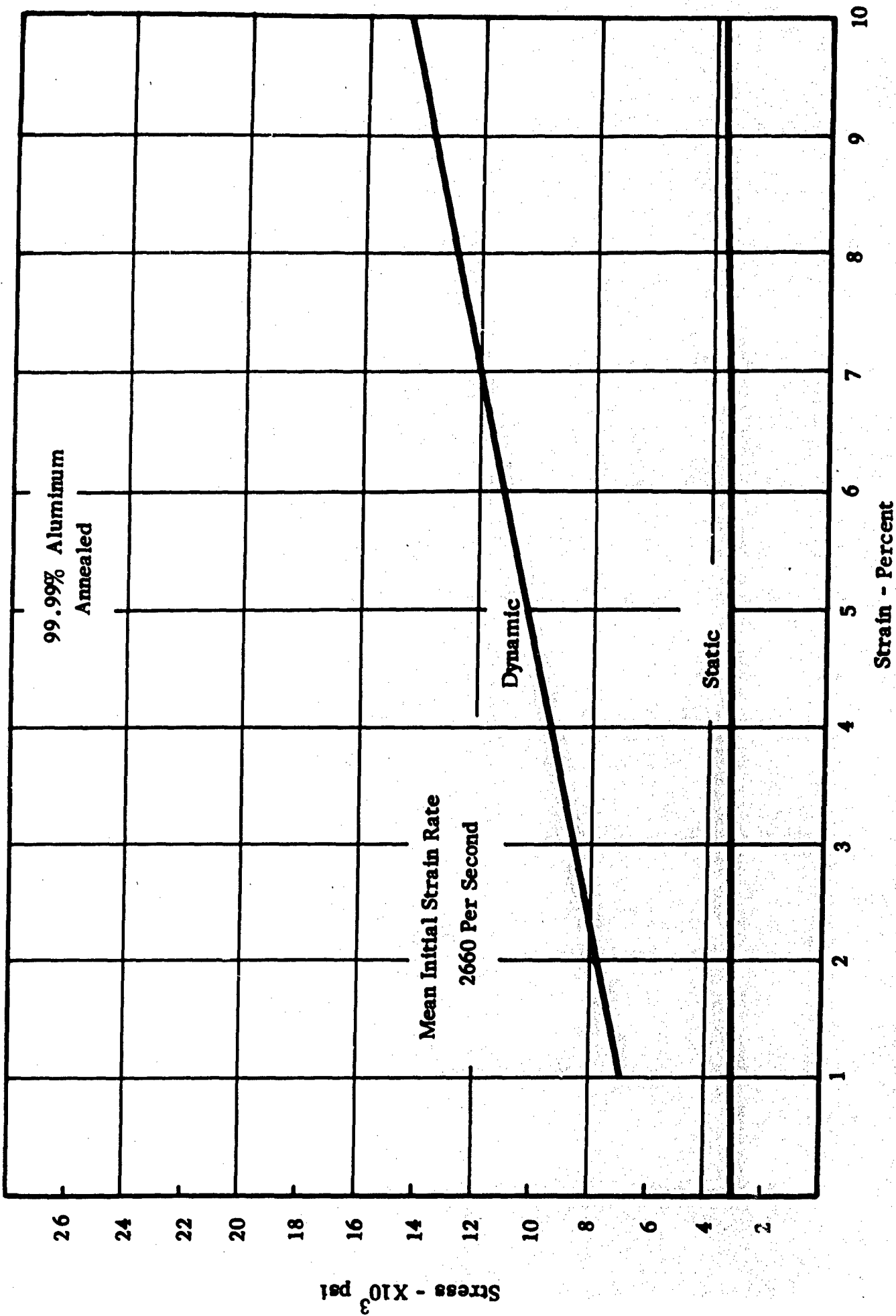


FIGURE 3 STRESS-STRAIN RESULTS-99.99% ALUMINUM

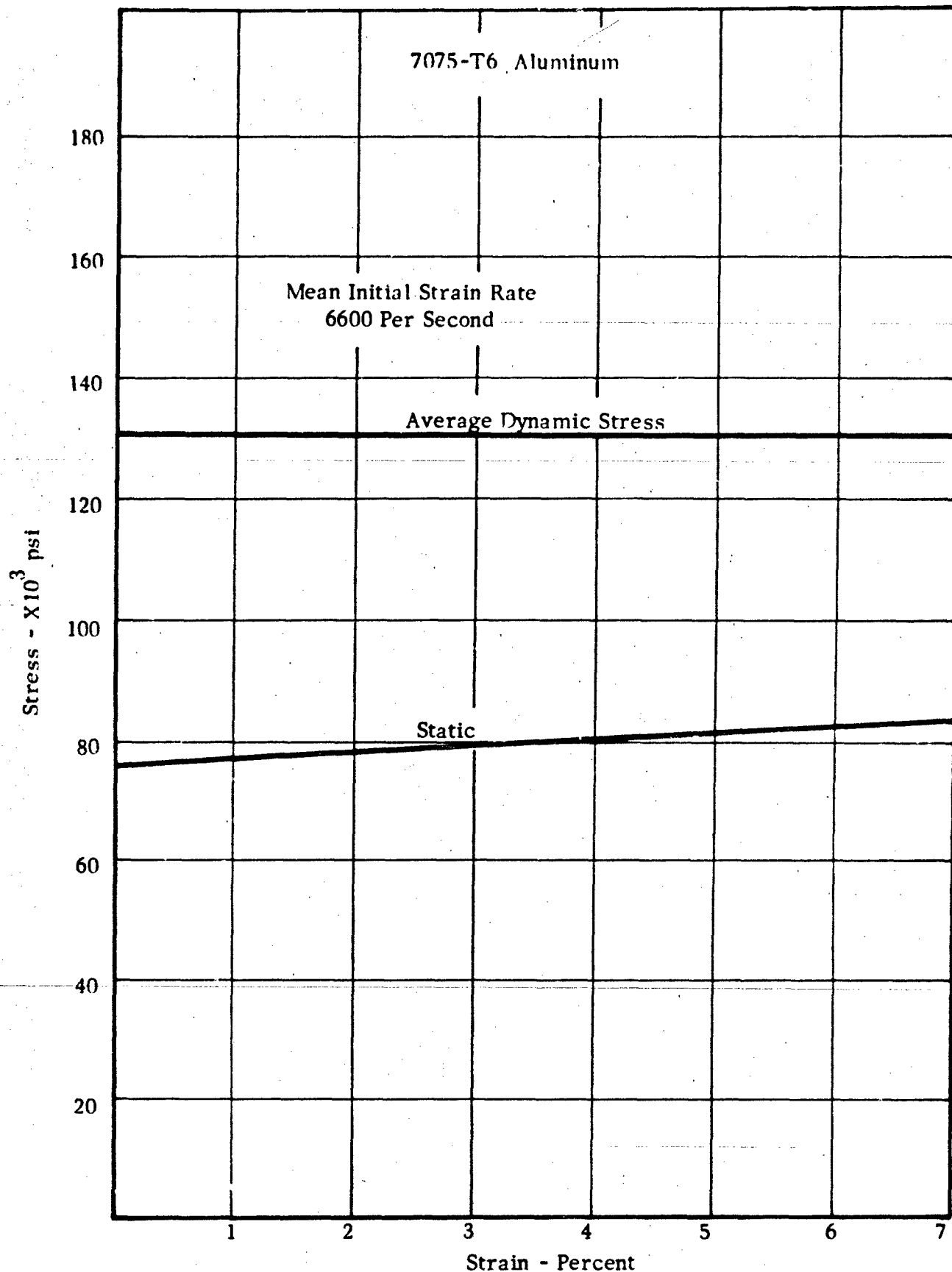


FIGURE 4 STRESS-STRAIN RESULTS-7075-T6-ALUMINUM

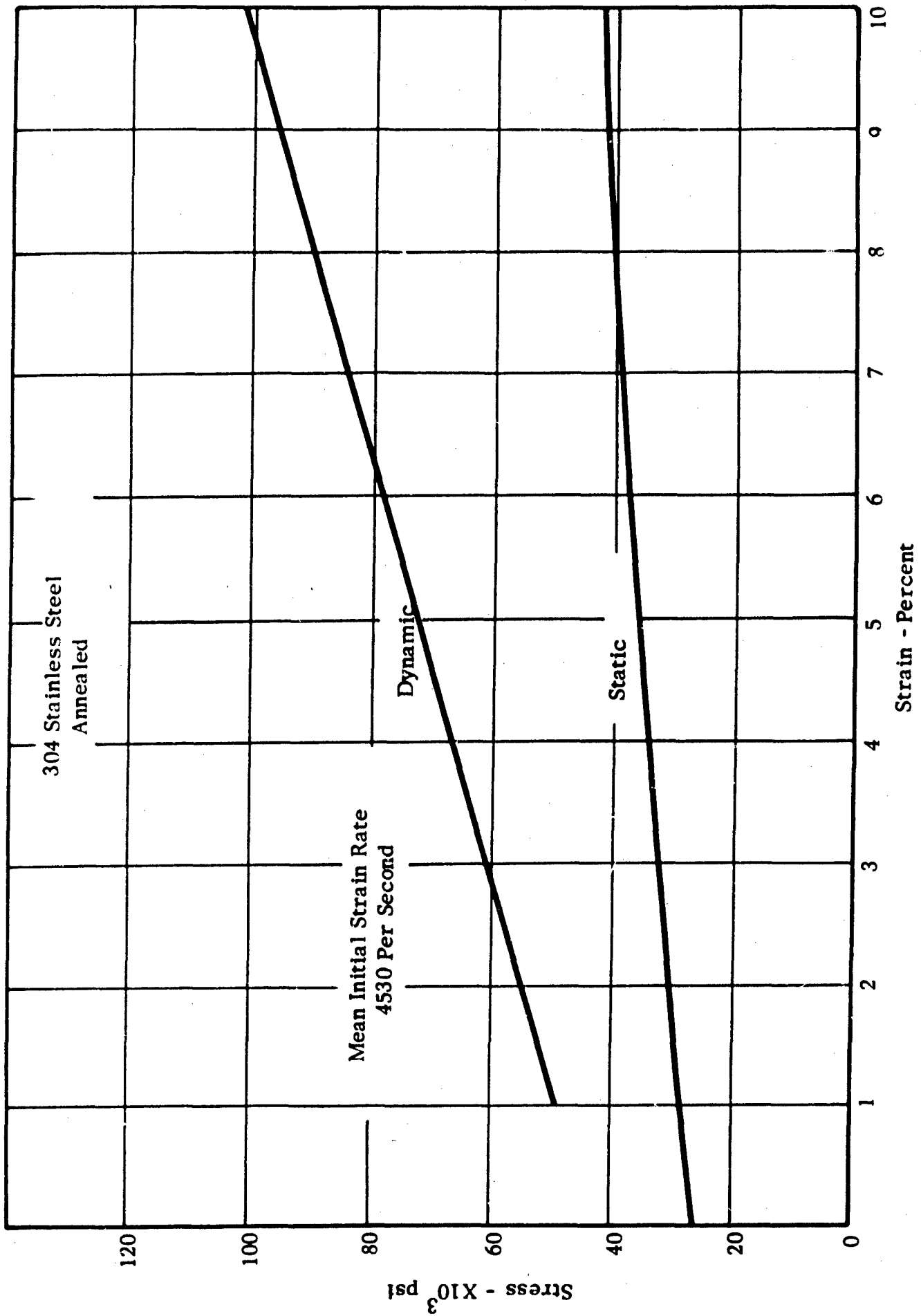


FIGURE 5 STRESS-STRAIN RESULTS-304 STAINLESS STEEL

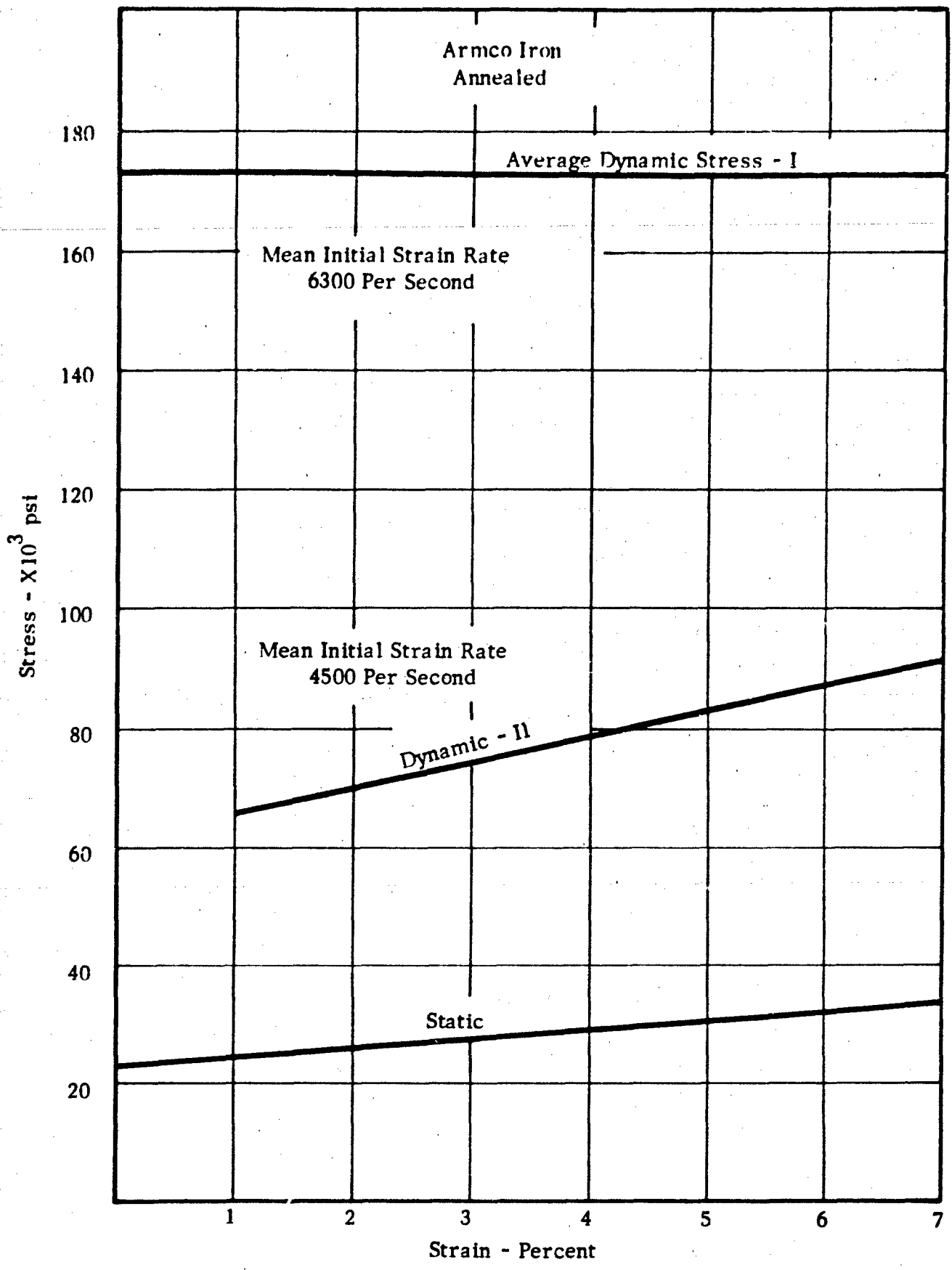


FIGURE 6 STRESS-STRAIN RESULTS-ARMCO IRON

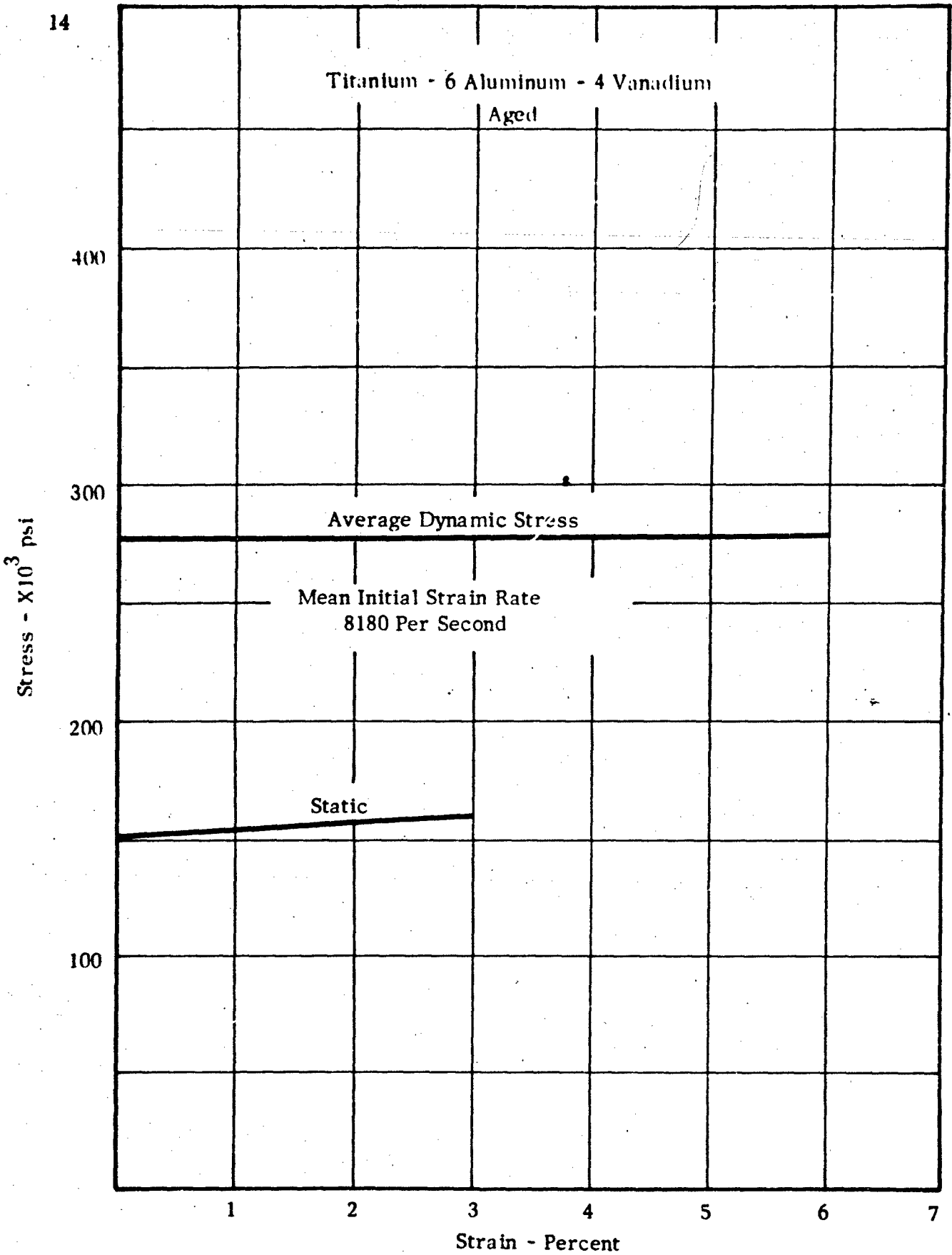


FIGURE 7 STRESS-STRAIN RESULTS-TITANIUM-6 ALUMINUM-4 VANADIUM

III. DUCTILITY AT HIGH STRAIN RATES

One of the more important factors in high energy rate forming processes is the ductility of the material under the conditions of the operation. It is also one of the factors over which there is a large amount of disagreement among the users of the process. It is apparent that the ductility of a material at high rates of strain is influenced not only by the flow behavior of the material but also by the mechanics of deformation in the particular piece being formed. In other words, identical pieces of material might fail in a ductile manner at quite different levels of strain if the plastic stress wave patterns involved in the forming operation are quite different. This is the probable source of a large part of the inconsistencies which have been observed in high strain rate ductility.

As in the case of the plastic flow properties, it is advantageous to separate the effects of the strain rate and the deformation mechanics. An understanding of the ductility of materials at high strain rates in the absence of plastic stress waves is an essential first step in the study of the total problem. The ring technique lends itself to such a study. By providing sufficient initial energy to the ring so that it expands to failure, it is possible to measure the elongation to failure under conditions of homogeneous, uniaxial stress. It is a system which can be meaningfully compared to a standard tensile test.

The parameter chosen to define the ductility of the materials in this study was the uniform elongation to failure rather than the total elongation, since the uniform deformation obtainable is more important in forming operations than the total elongation. Total elongation values include the deformation due to plastic instabilities, or necks, while forming operations are not normally carried out to the point at which such instabilities develop.

The experimental technique was a slight modification of that used for the flow curve work, with no photographic monitoring of the test. The core material was almost always 4340 steel hardened and tempered at 1100° F. A number of techniques were tried to allow the use of the larger charges required to cause failure of the ring, without causing break-up of the core. The technique which was the most successful involved omission of the shoulder on the core and the use of heavy 304 stainless steel sleeves on each end of the core. These sleeves were slipped part way down each end of the core, but not so far that they contacted the ring. These sleeves helped absorb the energy of the shock wave in regions away from the core, and also helped hold the core together if it failed. A number of explosive charge configurations were tried. The most dependable appeared to be a fairly large central charge, as in the plastic flow curve work, but detonated from each end by seismic detonators connected to a 5000 volt power source.

The strain was measured by means of a grid deposited on the rings. The grid was either vacuum-deposited copper or dyed Photo-Resist, although the latter proved more durable in these tests. The grid consisted of a series of seventy-two radial lines and four concentric circles on the top and bottom surfaces of the ring. The strain values used were taken from the uniform regions between necks and fractures on the expanded rings. The values obtained were quite uniform and reproducible from test to test on a given material. The low strain rate values were obtained on tensile specimens from a photo-deposited grid. Details of the experimental technique are given in the Second Interim Report (WAL TR 11.2/20-1) and the Sixth Interim Report (WAL TR 11.2/20-5). Detailed description of the materials used, their treatment, and low strain rate properties can be found in the Fourth Interim Report (WAL TR 11.2/20-3).

The results for those materials which gave significant ductility values are given in Table I.

TABLE I

UNIFORM ELONGATION TO FAILURE

<u>Material</u>	<u>Condition</u>	<u>Y. S. Ksi</u>	<u>Static Elong. % 10⁻³/sec</u>	<u>Dynamic Elong. % 10⁴/sec</u>	<u>Dynamic/ Static</u>
4340 Steel	Tempered 800°F	208	2	9	4.5
1100 Al	Cold Worked	15	6	19	3.2
T1-6Al-4y	Aged, 1100°F	150	3	9	3.0
4340 Steel	Annealed	76	11	13	1.2
1100 Al	Annealed	4.5	24	26	1.1
1015 Steel	Annealed	32	26	18	0.7
Armco Iron	Annealed	22	31	21	0.7
304 Stainless Steel	Annealed	58	46	24	0.5

There were three other materials tested for high strain rate ductility. These results are not included because of apparent changes in the failure characteristics at the high strain rates. 7075-T6 aluminum appeared to fail by shear at the high strain rates rather than by necking. A tungsten-7.5 nickel-2.5 copper alloy which exhibits good ductility at low strain rates failed by fracture along grain boundaries at very low strains under dynamic conditions. René 41 rings fractured in a brittle manner on planes parallel to the ring cross-section and to the plane of the ring. This appeared to be due to faults in the material we used and in the machining of the rings.

The number of necks and failures in these rings seemed to vary randomly from test to test. The elongation in the uniform regions appeared to be independent of the number of necks which formed. The elongation in the uniform regions of a 304 stainless steel ring was the same for a ring with an artificial neck machined into it before the test as it was for a normal ring. A ring which had been cut completely through before a test had necked regions elsewhere in the ring after the test.

It appears that a certain level of uniform strain can be accomplished in the rings independent of the formation of a few necks in the ring. But additional deformation cannot take place in the uniform region without the creation of a new neck in that region. It appears that additional uniform elongation and necking are occurring simultaneously in the ring after the initiation of the first neck at some finite strain. We cannot determine the sequence of events in tests such as these without high speed photographic observation. Our tests do not give us any definite information on the causes of necking or on the stress waves, if any, which these necks initiate into the rest of the ring.

Another interesting effect which we observed involved the hardness changes on 4340 steel in the hardened condition and annealed 304 stainless steel which resulted from high rate deformation of rings to failure. We measured the microhardnesses of tensile specimens and ring specimens before and after deformation to failure. The hardnesses were measured on the cross-sectional planes of these specimens. The results are given in Table II.

TABLE II

HARDNESS OF 304 AND 4340 STEELS - V.P.N.

<u>Material</u>	<u>Tensile Undeformed</u>	<u>Ring Undeformed</u>	<u>Tensile Deformed</u>	<u>Ring Deformed</u>
304 Stainless Steel	271	282	441	456
4340 Steel	494	463	549	469

The hardness change as a result of the deformation is about the same for the 304 ring and tensile specimen. This is despite the fact that the tensile elongation was very much greater than the ring elongation. The 4340 steel hardnesses are even more interesting. The tensile specimen deformed uniformly about 2 percent and showed a 50 point hardness increase. The ring, however, although it elongated uniformly almost 9 percent, had essentially no hardness increase. The temperature rise in the ring tests is not large enough to account for this lack of hardening.

IV. THE HIGH ENERGY RATE FORMING PROCESS

A. GENERAL

Under this heading we include all those process variables which do not specifically deal with the high strain rate behavior of the material in the absence of stress waves. The initiation, propagation, and interaction of plastic stress waves are intimately related to the geometry of the piece and the design of the forming operation. We include here also the design variables, such as the energy source and its configuration, the energy transfer medium and its configuration, the energy transfer process, die design, and of course, the deformation mechanics involved in the forming of the piece.

These factors were discussed in some detail in the Third Interim Report (WAL TR 11.2/20-2) on the basis of our own experience and the information supplied by other investigators. At that time we noted that one of the process variables about which very little was known was the nature of the energy transfer process by a pressure wave from the transfer medium to the work piece. The process appeared too complex to lend itself to analysis using the theories of wave propagation and transfer interfaces. We, therefore, have carried out an experimental investigation of the process as a part of this program. Since this work has not previously been reported, it will be described in some detail here.

B. INTERFACE ENERGY TRANSFER

One of the most interesting problems connected with high energy rate forming methods relates to the means by which, and the extent to which, energy carried by the shock wave is transferred into the blank. Obviously, our ability to design the process to provide a predetermined amount of forming is directly related to our ability to determine the amount of kinetic energy transferred to different parts of the blank. One part of this question is related primarily to the geometry of the forming system, the placement of the charge and other such matters which are generally susceptible to analytical treatment. Another very important part of the problem, however, is the extent to which the energy carried by the shock wave is transferred to the blank, relative to the amount which is reflected from the water-blank interface. If the transfer medium were another metal, we could calculate the amount of energy transferred across a given interface. By using impedance data for the two metals, we can readily calculate the percentage of the wave which will propagate across an interface and that amount (the remainder of the incident wave) which will reflect from the interface. We can, in principle, make this calculation as readily for water-metal systems as we can for systems involving two metals. In the latter case, we make the

(ordinarily accurate) assumption that the front piece will separate from the back piece as soon as the wave has reflected from the free surface and returned to the original interface, at which time a tensile component across the interface is induced. This is equally the first step in a system involving a shock wave propagating from water into a metal. In both cases, as soon as the front blank separates from the rear material, a new reflection occurs at the free surface of the rear material which doubles its particle velocity at that point. Water is so much more compressible a material than the metals under consideration that a given shock pressure induces in water a much higher particle velocity than in metals. Therefore, even though the shock wave pressure has been reduced considerably by the loss of the front pellet, which has, of course, trapped the high pressure portion of the shock wave, the water may still be able to accelerate to a velocity sufficient to overtake the metal fragment. If this happens, and it contacts the metal again, the wave can once again propagate into the metal and the sequence will be repeated over and over again until the difference in magnitude becomes so large that it is no longer possible for the surface of the water to accelerate to a sufficient velocity. Furthermore, this argument may plainly be applied to differential motions with the result that a shock wave propagating in water may be able to transfer practically all of its energy to a metal blank. This problem seems so central to an understanding of the mechanics of HERF processes, that an experiment was designed to investigate this possibility.

A schematic of the experimental apparatus is shown in Figure 8. It consists, essentially, of three sections. The center, of course, is the water transfer fluid, the end labeled "impact block" is that end where the shock wave is induced, and the pellet shown at the opposite end is the free blank whose velocity we wish to observe. An impact technique was chosen to initiate the shock wave for several reasons. First, the alternative, that of using a small explosive charge or a blasting cap, involves the necessity for relatively elaborate safety precautions. Secondly, it seemed easier to make reproducible impact shocks over a relatively wide range of pressures than would be the equivalent operation using blasting caps, especially if we were limited to commercial sizes.

The water column itself, of course, must meet certain geometrical requirements. If the length/diameter ratio is greater than about 1, then the shock wave from that point onward has essentially been reduced by lateral rarefactions to a non-steep front acoustic wave. This represents an entirely different system and is, therefore, not pertinent to the high energy rate forming methods which we wish to investigate. As for the pellet, we could, of course, simply use an end plate of appropriate material and measure its velocity. However, there are two reasons for going to the pellet design. In the first place, since we are not generating a plane wave, any end piece of a size comparable to the wave radius will sense different particle velocities and different pressures at different radii and will, therefore, accelerate non-uniformly. This will lead to plastic deformation, thereby absorbing part of the energy which has been imparted to the

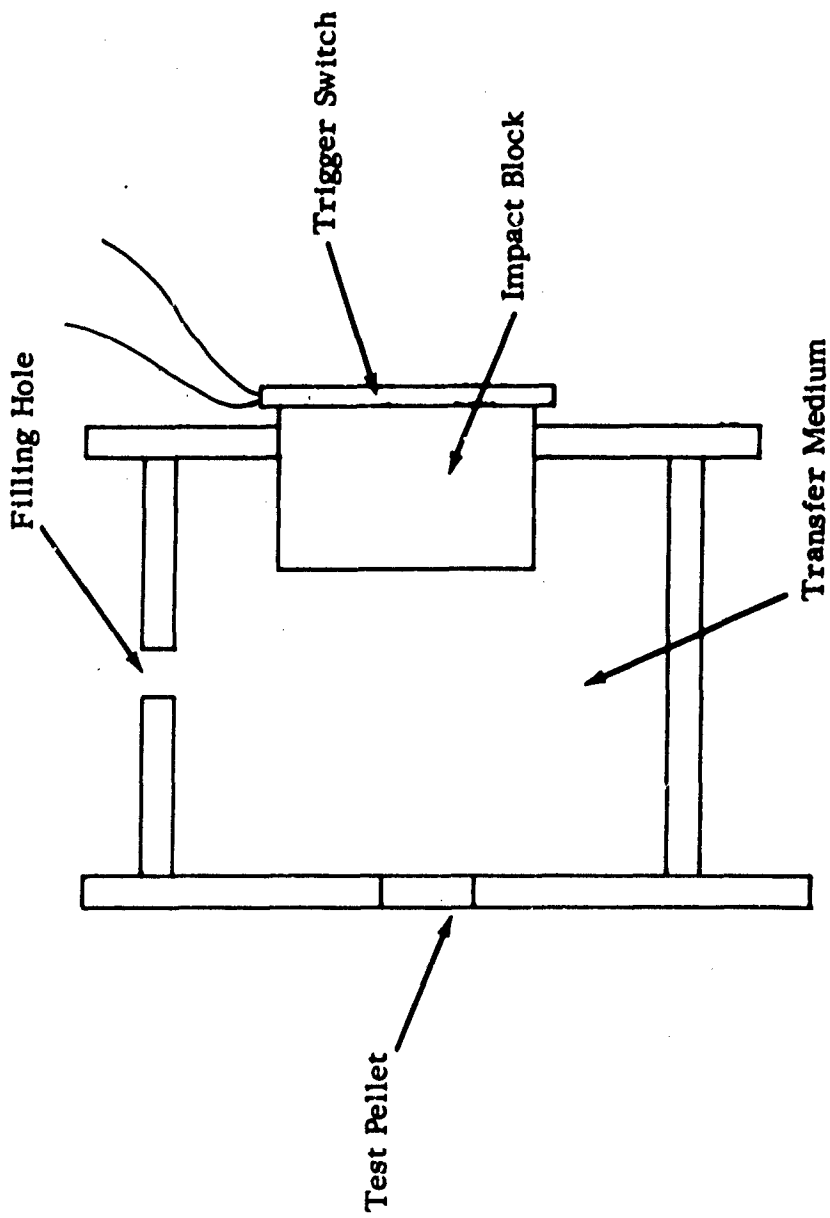


FIGURE 8 EXPERIMENTAL APPARATUS INTERFACE ENERGY TRANSFER

blank by the shock wave. Moreover, we would prefer to avoid end constraints for similar reasons. To avoid these problems, we have used an inserted free pellet which is sufficiently small so that, to a first approximation, the pressure acting across its face is uniform. Since it has no fixed constraint, its velocity is not reduced except by the slight friction at the walls. The pellet material used was aluminum, primarily because of the excellent shock propagation and impedance data available. The impact itself was delivered by a bullet, since this seemed to offer the simplest technique. The only requirement on the impact block is that it not be punctured or appreciably deformed (on the water side) by the impact. If this condition is not met, extremely non-uniform waves are generated which cannot properly be analyzed. The impact block material used was fully hardened 4340 steel, 1/2" thick, which was sufficient to completely stop the highest velocity bullet employed without any damage to the opposite face of the block. Figure 9 is a photograph of the experimental cell showing the impact block and the tubular aluminum chamber containing the water. The square piece on the front of the impact block is an oscilloscope trigger switch which is discussed below.

The cartridge used in this work was the caliber .243 Winchester. This is only one of many cartridges which could have been selected and no special properties of the .243 are involved in this work. The requirements were 1) a bullet which is relatively long compared to its diameter; 2) a relatively broad range of available velocities; and 3) substantial reproducibility of velocity for a given charge. Moreover, one would also like to use a cartridge with a commercially available range of bullet weights and shapes. In order to generate the cleanest shock wave for the present experiment, it was felt desirable to use a bullet having a flat end. This was also helpful in preventing penetration of the impact block. A number of experiments were tried in order to reach the best configuration. The one which ultimately gave the most reliable results was based on a 105 grain bullet manufactured by the Speer Products Co. This bullet, which was, of course, pointed to begin with, was machined off to a length of .725 inches and a weight of 87 grains. At this length a very slight amount of the initial chamfer of the bullet nose was still present to provide a lead into the rifling grooves. It was found that this particular bullet could very reliably be projected at velocities of 3000 ft/sec with great accuracy, did not keyhole in mid-air, and could generate appropriate shock waves. The powder charge finally selected for this bullet consisted of 42.0 grains of DuPont type 4350 rifle powder. In order to assure uniform velocities, and in order to check the accuracy of the loads, two velocity pick-ups were mounted in the line of the bullet. These consisted of simple photocell-interrupted beam units. During the development of the bullet and the particular load, velocities were measured on every shot using the pick-up indicated and a Beckman-Berkeley digital counter. The final results indicated that these bullets could be machined down, loaded with powder, and fired to give a velocity of 3050 ft/sec plus or minus 20 ft/sec. Lead at this velocity impacting steel will yield a maximum shock pressure of approximately 160 kilobars.



FIGURE 9 EXPERIMENT 9 CHILL

Arthur G. Clarke, Inc.

A capacitive technique was used to measure the velocity of the pellet. Ordinarily, capacitive methods measure displacement as a function of time. In the present case, it seemed much more desirable to measure velocity directly. Every additional folding of the shock wave to induce more velocity in the pellet would show up as a staircase in the velocity-time trace instead of as a change in slope, which is much more difficult to observe. The circuit diagram for the pick-up is shown in Figure 10, and a photograph of the apparatus in Figure 11. The rear electrode is mounted on a micrometer screw so that it may be readily adjusted to a known spacing for different experiments. This is also an aid in calibration of the pick-up. The only circuit difference between this and a displacement technique is in the choice of components. In this case, the capacitance of the transfer capacitor is so small compared to the total system capacitance that it, in conjunction with the resistor, acts as a differentiating circuit and provides a velocity input for the oscilloscope. Analysis of this circuit leads to the following exact expression for the voltage output V , at a time t , as a function of the circuit parameters and the desired velocity, dx/dt .

$$V(t) = R \left[\left\{ E - V(t) \right\} \frac{dc}{dx} \frac{dx}{dt} - \left\{ C(t) \right\} \frac{dV}{dt} \right]$$

Since $V(t)$ is very small compared with E , the applied voltage, and since dV/dt is small in the early stages of motion where our major interest lies, we can approximate this equation as follows:

$$V = RE \frac{dc}{dx} \frac{dx}{dt}$$

or rearranging to solve for $dx/dt = v$, the velocity,

$$v = \frac{V}{RE \, dc/dx}$$

R and E are obtained directly from the circuit, dc/dx can be calibrated in advance, and V is read from the oscilloscope trace. Notice that the equation indicates that if a constant velocity is induced, the output will show an exponentially rising voltage characteristic. It is, therefore, rather tedious to determine the exact velocity except at the initial spacing. It is possible, by stepwise integration, to solve for the velocity at any point. In the present experiments, however, this was not felt to be a serious disadvantage since we were not so much interested in precise velocity parameters as in relative changes in velocity. In order to calibrate the system, we require the value of dc/dx . This was measured with a capacitance bridge at a variety of spacings adjusted by the micrometer screw. This approximate calibration, for the standard initial spacing of .012 in., leads to a value of the velocity, in feet per second, as being equal to about .4 times the voltage output in millivolts. In order to expand the scale on the oscilloscope

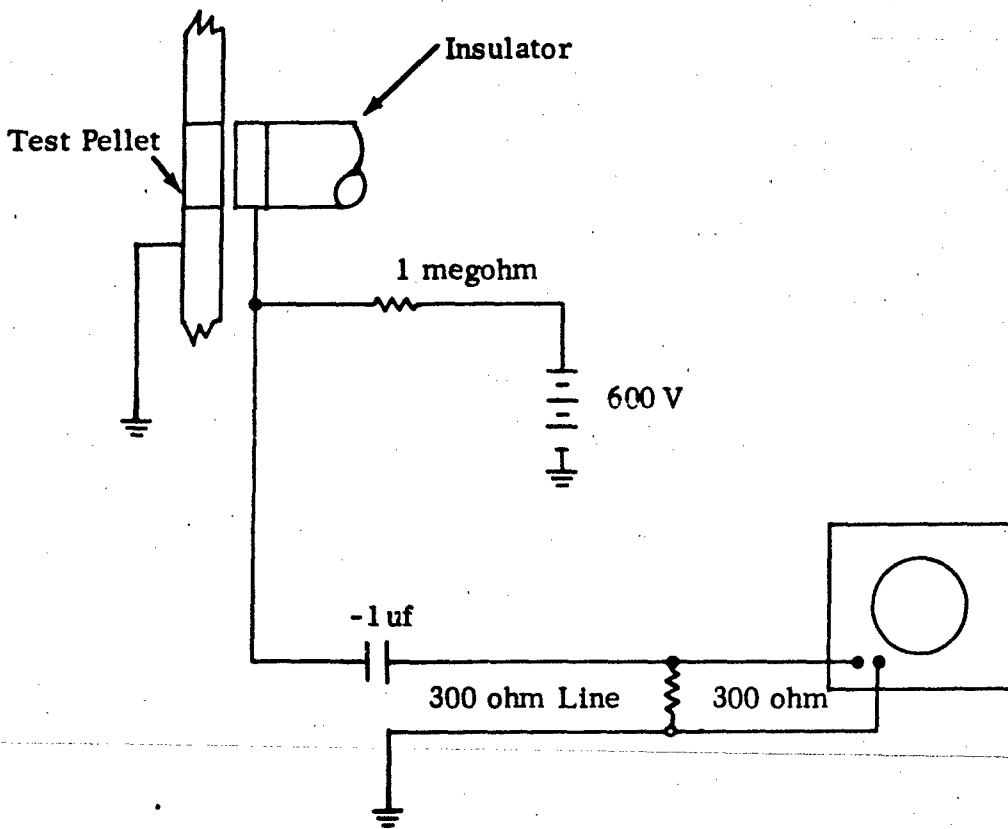


FIGURE 10 SCHEMATIC OF VELOCITY PICKUP

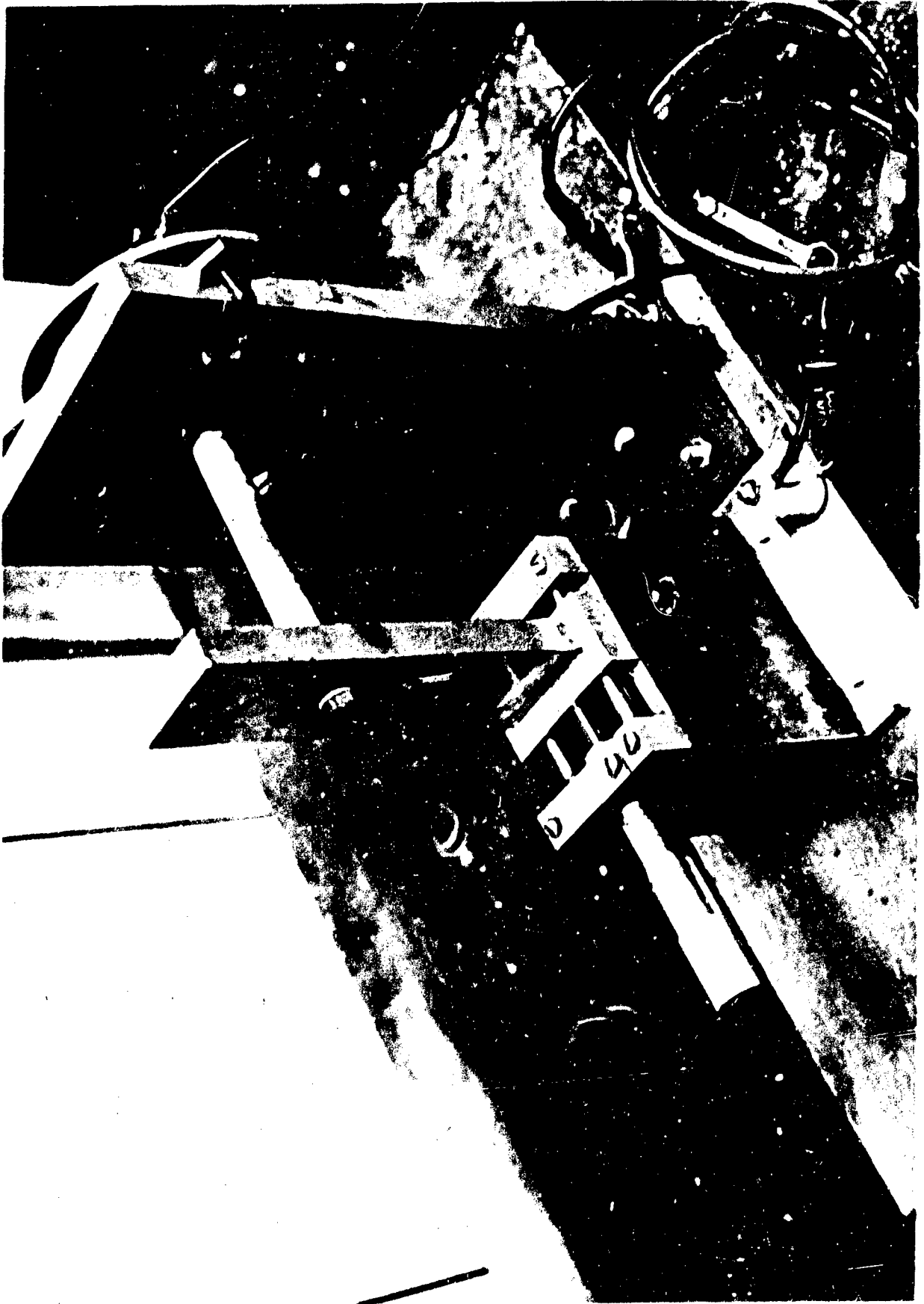


FIGURE 11 VELOCITY PICKUP APPARATUS

and get the most accuracy possible, it was necessary to find some means for triggering the scope upon impact of the bullet. If the velocity pick-ups had been used the time delay between that position and the final impact would have been so large that the time scale needed to observe the passage of shock waves through the pellet would have been compressed into a very small portion of the oscilloscope trace. A postage stamp switch was therefore added to each experiment, as can be seen in Figures 8 and 9. This device consists simply of a piece of paper, with a hole in it, across which two pieces of aluminum foil are taped. They are used as a switch acting in series with a battery and the trigger input of the scope. The bullet short circuits the two aluminum foils and therefore completes the circuit. This was a very reliable device, which enabled the oscilloscope trace to be expanded to a point where a reasonable time scale could be obtained.

A photograph of the oscilloscope trace for a typical experiment is shown in Figure 12. In this case, at least twelve separate velocity steps can be observed, indicating that the shock wave has transferred a much greater proportion of its energy to the pellet than one would have predicted. This experiment used a water column 1" long, with a 1/8" aluminum pellet. In contrast, Figure 13 shows a similar photograph using an experimental set up in which the water was replaced by a block of aluminum. In this case, only one velocity pulse can be observed, as was predicted. The initial small pulse is due to the elastic precursor wave, which is of very small amplitude compared to the main shock front which follows. The effect of different lengths of water in the column is only to change the pressure of the shock wave reaching the pellet and, ultimately, to limit the number of velocity steps which can take place. It therefore seems established that, under these circumstances, a shock wave propagating from water into a metal blank will reflect a number of times inside the blank and induce a much greater velocity in the blank than would be predicted from a single transfer step. One other experiment was performed in an attempt to demonstrate the reflection of the shock wave back and forth inside the pellet. In this case the water column was replaced with a piece of steel and one of the 1/8" aluminum pellets was merely attached with lubricating oil on the outer surface of the block. Under these circumstances, when the pellet leaves the block, it is acting as an internal third plate between two plates of a capacitor and analysis of the circuit indicates that the voltage output, as a function of velocity, will increase as the pellet reaches the center of the space and then decrease symmetrically. The output is also proportional to motion of both faces of the pellet and it should therefore be possible to observe peaks corresponding to the reflection of the wave back and forth inside the pellet. The results of this experiment can be seen in Figure 14 and indeed there is a spacing of approximately 2.8 microseconds between adjacent major peaks. The velocity of longitudinal sound waves in brass is approximately 15,400 ft/sec, and if one calculates the time required for an elastic wave to travel from one side of a 1/4" pellet to the other, a time of 2.6 microseconds is indicated. This corresponds quite well to the measured value on the photograph.

An explosive forming system utilizing a water transfer fluid to transfer the shock wave from the explosive source into the blank to be formed actually transfers energy to a much greater extent than would have been predicted from the more usual kinds of analysis. In fact, it may be fairly accurate to assume that most of the energy that reaches the interface is transferred into the blank, and that the amount reflected is only a relatively small proportion of the initial wave.

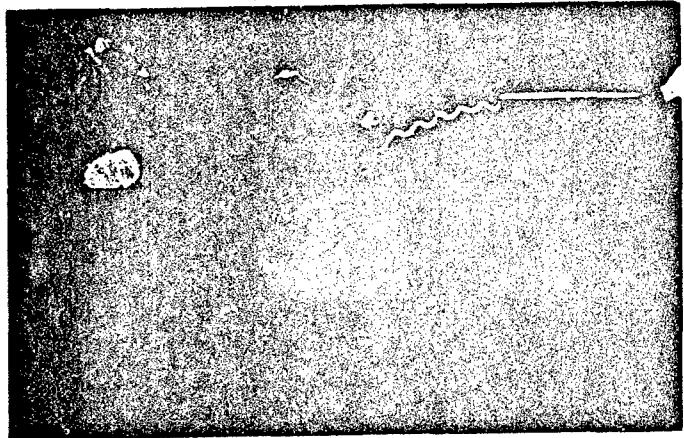
t ←

FIGURE 12 WATER-ALUMINUM
TRANSFER

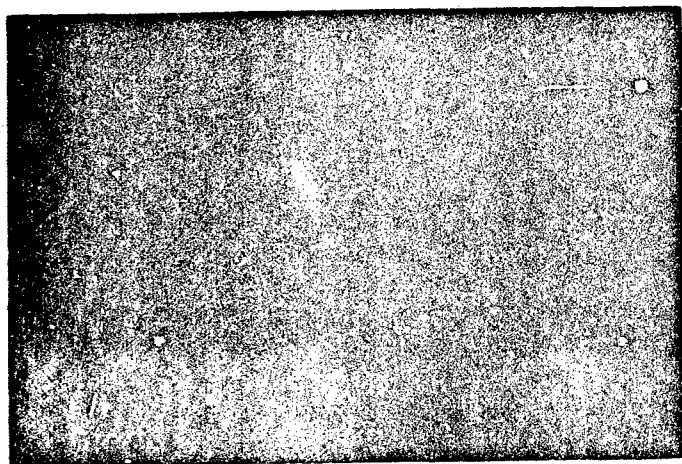


FIGURE 13 ALUMINUM-ALUMINUM
TRANSFER

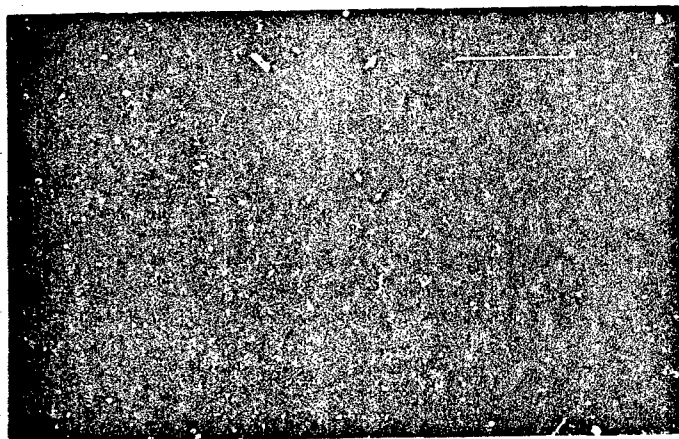


FIGURE 14 WAVE REFLECTION
TRACE

V. FUTURE EFFORTS

This program has provided the first steps toward an understanding of high energy rate forming processes. It has by no means provided all the information that will be necessary for intelligent process design. It has however, clarified the directions which future work should take. It has also become apparent as a result of this work, that some areas in which considerable effort is presently being expended will probably not contribute in a significant way to the desired process design goals.

The first stage in future investigations should involve completion of the study of the dynamic behavior of materials under a biaxial stress system. During the present program, an experiment which can be used to provide this information was designed and tested (tube expansion). This experiment should be utilized to provide the same types of information that were produced by the ring experiment; that is, stress-strain and uniform elongation to failure data.

The second stage should apply the information generated with the uniaxial and biaxial stress system studies to an investigation of a real forming operation involving wave propagation. In the initial stages, this work should be confined to a system in which wave propagation and interaction considerations are relatively simple. The most promising technique would appear to be a cupping operation which derives its energy from a plane, longitudinal shock wave. Known from the previous work, the dynamic behavior of the material, one can determine the stress levels in the plate as a function of position and time by monitoring the strain in the plate throughout the process.

The final stages of the work should be concerned with systems which do not have the geometrical simplicity of the plate and plane wave configuration described above. This would involve both non-planar energy inputs and more complex geometrical shapes.

A modest amount of work in this final stage should permit the establishment of an analytical model for high energy rate forming processes. This model would permit intelligent design of the process for all but the most unusual forming operations. In particular, it would permit design of the process so that parts can be formed with little transfer of energy to the die. This appears to be a much more fruitful approach to the die problem than that of designing massive dies which can repeatedly absorb large amounts of excess energy. A large part of the cost of HERF processes is presently associated with die design and construction.

Finally, the model which results from such investigations would lead, at least in principle, to a partial solution of the problem of scaling up to very large sizes. It seems evident that the future of HERF processes lies, at least partially, in their use as a method for forming such pieces. The problem of scaling is, in general, extremely complex, but the first step in obtaining design procedures for large pieces must come from an understanding of the process on the more modest, but successful, scale in which it is currently being employed.

REFERENCES

- 1) T. von Karman, "On the Propagation of Plastic Deformations in Solids," NDRC Report A-29, OSRD 365, January 1942.
- 2) G. I. Taylor, "The Testing of Materials at High Rates of Loading," Journal of the Institute of Civil Engineers, Vol. 26, 1946, p. 486.
- 3) K. A. Rakhmatulin, "On the Propagation of the Unloading Wave," Prikl. Mat. Mekh., Vol. 9, No. 1, pp.91-100, 1945 (in Russian).
- 4) L. E. Malvern, "The Propagation of Longitudinal Waves of Plastic Deformation in a Bar of Material Exhibiting a Strain-Rate Effect," Journal of Applied Mechanics, Vol. 18, p. 203, 1951.
- 5) J. F. Bell, "Determination of Dynamic Plastic Strain through the Use of Diffraction Gratings," Journal of Appl. Phys., Vol. 27, No. 10 p. 1109, 1956.
- 6) E. A. Ripperger and C. H. Karnes, "Plastic Impacts on Short Cylindrical Specimens," Dynamic Behavior of Materials, ASTM Special Publication No. 336, 1963.
- 7) F. E. Hauser, J. A. Simmons, and J. E. Dorn, "Strain Rate Effects in Plastic Wave Propagation," Response of Metals to High Velocity Deformation, Interscience Publishers, New York, p. 93, 1961.
- 8) H. Kolsky, Proc. Phys. Soc. (London), Vol. 62, p.677, 1949.